SKBF
KBS
TEKNISK
RAPPORT
82-24

Migration model for the near field
Final report

Göran Andersson
Anders Rasmuson
Ivars Neretnieks

Royal Institute of Technology
Department of Chemical Engineering
Stockholm, Sweden, 1982-11-01

SVENSK KÄRNBRÄNSLEFÖRSÖRJNING AB / AVDELNING KBS

POSTADRESS: Box 5864, 102 48 Stockholm, Telefon 08-67 95 40

MIGRATION MODEL FOR THE NEAR FIELD

Final report

Göran Andersson
Anders Rasmuson
Ivars Neretnieks

Royal Institute of Technology
Department of Chemical Engineering
Stockholm, Sweden 1982-11-01

A list of other reports published in this series during 1982, is attached at the end of this report. Information on KBS technical reports from 1977-1978 (TR 121), 1979 (TR 79-28), 1980 (TR 80-26) and 1981 (TR 81-17) is available through SKBF/KBS.

ROYAL INSTITUTE OF TECHNOLOGY
Department of Chemical Engineering

MIGRATION MODEL FOR THE NEAR FIELD
Final report

Göran Andersson
Anders Rasmuson
Ivars Neretnieks

1982-11-01

SUMMARY

The near field model describes the transport of substances dissolved in the groundwater to and from a canister in which radioactive materials are stored.

The migration of substances that can cause corrosion (oxidants) of the canister is described by means of a mathematical model. The model takes into account diffusion through the buffer material and water flow in the rock fractures. The oxidants are carried by the groundwater in the fractures up to the clay barrier and then diffused through the buffer material to react finally with the canister material. Two distinct transport resistances can be distinguished in this transport process. The first consists of the diffusion resistance in the buffer material and the second arises due to diffusion resistance in the flowing water in the thin fractures in the rock. The two transport resistances have been calculated under steady-state conditions for three-dimensional geometry.

The waterbearing fractures in the rock are modelled as equidistant and situated in parallel planes perpendicular to the longitudinal direction of the canister. The flow is described by potential flow. In the calculations, the resistances have been calculated separately and then added to obtain a total resistance using the formula:

$R_{TOT} = R_L + R_V$

R_L, R_V denote the resistances in the buffer material and between the buffer material and the groundwater (s/m^3)
($R = 1/kA$)

k = mass transfer coefficient (m/s)

A = diffusion area (m^2)

Calculations have also been performed where the diffusion in the flowing water in the fractures and the diffusion in the clay barrier have been calculated simultaneously. These calculations produce results in agreement with those where the resistances have been calculated separately. The former method is much more computer-time-consuming, however.

This model for the inward transport of oxygen has also been compared with the simplified model used in KBS TR 79. The agreement between these models is very good. Both models show that the resistance in the buffer material is of less importance for the total resistance.

The model can also be used to calculate the non-steady-state phase of the inward or outward transport of dissolved species.

The model has also been used to calculate how a redox front caused by radiolytically produced oxidants moves out through the clay and into the rock. It has been shown that the

migration rate of the redox front can be calculated with good accuracy by means of simple mass balance computations, except where very short times are involved.

The transport of radiolytically formed hydrogen away from the fuel has been calculated. When dissolved in the water, hydrogen can be transported through the clay barrier by means of diffusion without the partial pressure of the hydrogen exceeding the hydrostatic pressure.

Calculations have been performed to ascertain whether the inward transport of water through a hole in the canister can be a limiting factor for radiolysis. The possibility that even small holes can transport significant quantities of water cannot be ruled out.

CONTENTS

1. INTRODUCTION

Final storage of the radioactive waste from the Swedish nuclear power plants is to take place deep down in the bedrock. The repository consists of a tunnel system excavated at a depth of 500 m in rock of very low permeability. The waste is first enclosed in canisters of some corrosion-resistant material, for example copper, after which these canisters are placed in holes drilled in the floors of the tunnels. The space between the canister and the rock is filled with highly compacted bentonite clay. The purpose of this clay is, among other things, to raise the diffusional resistance for migrating substances and impede, through its low permeability, direct contact between the canister and the flowing groundwater, protect the canister mechanically and also serve as a sorbent for certain radionuclides.

When the tunnels have been finally sealed by being filled with a mixture of sand and bentonite, the question arises: How long will the canisters remain intact? This is dependent partly on how rapidly corrosive substances (oxidants) can be transported into the canister and partly on whether corrosion will take place evenly over the entire canister surface or will be concentrated to small areas, a process known as pitting. An estimate of the magnitude of the oxidant transport can be obtained with the aid of a mathematical model. The extent of pitting must be based on experimental data, since no theories exist concerning its origin and progression.

When the canister has been penetrated, water will enter and leach out the spent fuel. The radionuclides that escape in this manner will then start to migrate through the clay

barrier and on out into the surrounding rock. Direct contact between the waste and the water also gives rise to α-radiolysis. Since some of the products that are thereby formed are highly oxidizing, the redox conditions in the vicinity of the repository may change from reducing to oxidizing. Even before the canister is penetrated, some radiolysis is caused by γ-radiation. This radiolysis increases sharply as the thickness of the canister decreases. The oxidizing substances migrate outward from the canister and form a moving front between a region with reducing conditions and a region with oxidizing conditions. The migration rate of the front is determined by the production rate of the oxidants and the quantity of reducing substances in the water and the rock. Some of the oxidizing substances created by radiolysis will also attack the canister material. This process has not yet been dealt with in detail.

The outward transport of radioactive substances dissolved in water from the interior of a damaged canister to flowing water in the rock is described in the same manner as the inward transport of oxidants.

Radiation from the radioactive substances causes radiolysis of the water. The water is thereby split into hydrogen and oxidizing substances, including hydrogen peroxide. The transport of the hydrogen away from the vicinity of the canister by means of flow and diffusion has been investigated, as has the reaction of the oxidizing substances with, above all, bivalent iron in clay and rock. In the million-year perspective, the oxidizing substances can, under certain conditions, form a region with oxidizing conditions up to several tens of metres from the canister. Outside of this area, the rock remains unaffected.

Mechanisms for the inward transport of water through the clay and through the corrosion products from the canister have been studied. It has not been possible to rule out the possibility that even small holes in the canister can allow so much water to enter that the supply of water will not be a limiting factor for the radiolysis. This is especially true for long periods of time when radiolysis is not so intensive. For short periods of time, the inward transport of water and the simultaneous outward transport of hydrogen will probably greatly reduce radiolysis.

2. INWARD TRANSPORT OF OXIDANTS TO THE CANISTER OR RADIONUCLIDES AWAY FROM THE CANISTER

The basic principle involved here is that the substances are transported from a region of high concentration to a region of low concentration. In the following, the transport of dissolved substances to a canister, where they are assumed to react rapidly with the canister material, is described. These reactive substances pass from the water to the canister. After a postulated breach of the canister, when the water comes into contact with the radionuclides, the radionuclides dissolve in the water. The transport then proceeds from the interior of the canister to the surrounding water. The difference between the two cases is merely in the direction of transport. Otherwise, they are described with the same mathematical equations. The description below pertains to the inward transport of reactive substances.

A prerequisite for the the corrosion of the canisters is that oxidants can be transported to the canister. If the oxidants are assumed to react immediately with the canister material, the corrosion rate is determined by how rapdily the inward transport can take place. The oxidants are assumed to be dissolved in the groundwater that flows in the rock fractures. From there, they are then transported via the clay barrier to the canister surface, where they are assumed to react instantaneously with the canister material (1).

Figure 2.1 shows how a fracture in the rock conducts water past the impervious clay in the hole. The oxidants flow with the water up to the clay. The hydraulic conductivity of the clay is very low ($K_p \leq 10^{-13}$ m/s) (2). This means that the transport of oxidants through the clay due to water flow through the clay is very low compared to the transport due

to molecular diffusion (3). The oxidant transport from the flowing water in the fracture to the canister can be described in the following manner. The flowing water brings oxidants up to the vicinity of the clay barrier. They diffuse from the groundwater towards the clay, into the clay and up to the canister surface. Here, they are assumed to react instantaneously with the canister material. Figure 2.2 illustrates this process schematically.

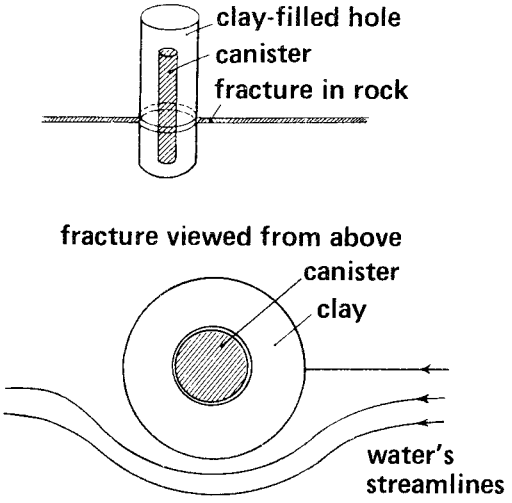

Figure 2.1 Canister with waterbearing fracture

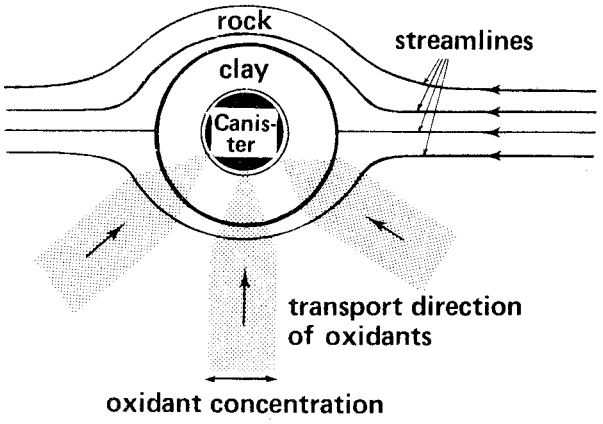

Figure 2.2 Transport of dissolved substances to the canister

The figure shows that the water in the fracture will be partially depleted of oxidant some distance out from the clay. The magnitude of this depletion depends mainly on how long a time it takes for the water to flow past the clay-filled hole.

In order to simplify the following discussion, the concept of "mass transfer resistance" is introduced here. This concept simplifies comparison of the importance of the different barriers. The mass transfer resistance is analogous to electrical resistance and thermal resistance and can be treated using similar formulas.

The mass transfer resistance R, can be written:

$$R = \frac{\Delta c}{N} \qquad (2.1)$$

where Δc is the driving force (concentration difference), N is the mass transferred per unit time. For flowing media such as the water in the fracture, an equivalent resistance can be calculated with the aid of the diffusion equation (Fick's laws). This is dealt with later on.

Two distinct transport resistances can be differentiated between the canister surface and the groundwater. The first arises due to diffusion in the flowing water. The second consists of the compacted bentonite clay barrier through which the oxidants must diffuse. The total resistance is then the sum of these two partial resistances. For the purpose of comparing with the results obtained in KBS TR 79, these resistances are calculated separately and under steady-

state conditions in one case. Calculations have also been performed for the case where the fracture and the clay are regarded as a continuous medium.

In order to make it possible to quantify the amount of oxidants transported in with a mathematical model, a number of assumptions must be made. These assumptions have principally been made within those areas where our present state of knowledge is deficient, such as the water flow in the fractures, but they have also been made for the purpose of simplifying the model. The most important assumptions can be summarized in the following points:

- The rock fractures are plane and perpendicular to the longitudinal direction of the canister and lie in parallel planes with constant spacing
- The canister is assumed to be infinitely long, i.e. end effects are neglected
- The flow in the fractures is described by potential flow
- Steady-state conditions prevail
- The influence of temperature gradients is neglected
- The bedrock is completely impervious to flowing water and to the oxidants.

Since the fracture spacing is assumed to be constant, planes of symmetry exist perpendicular to the longitudinal direction of the canister. Calculations therefore only have to be carried out for a region bounded by two such planes.

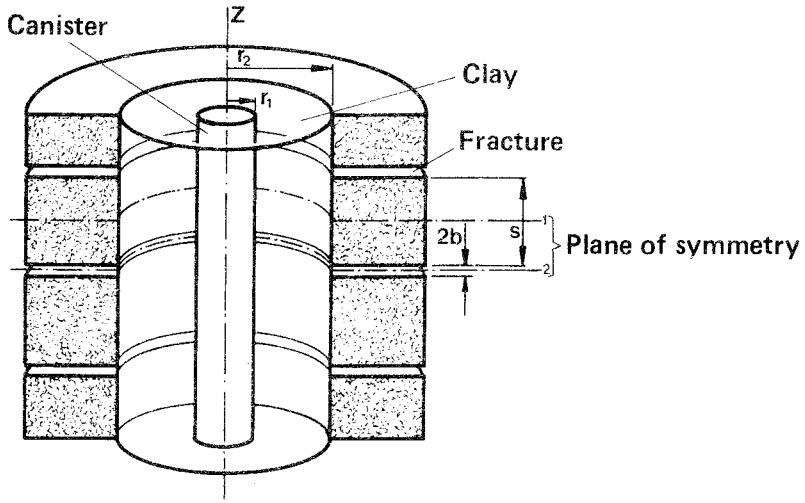

Figure 2.3. Definition drawing of the modelled system.

2.1 Coupled mass transport and flow in the fracture

The water flow and the mass transport can, in principle, be described rigorously in the combined system of fractured rock and clay fill in a hole in the rock. Navier-Stokes' equations are used for this purpose. They describe the flow and the continuity equation for both the water and components dissolved in the water. The continunity equation for dissolved components includes the transport mechanism of diffusion. We have chosen to make some simplifying assumptions in order to reduce the system to a more comprehensible and manageable form. The rock is assumed to consist of impenetrable blocks with plane-parallel fractures between the blocks. Flow in a fracture is described by potential flow. This is the usual assumption for slow flow in geologic media. These fundamental assumptions greatly simplify the picture. Mass transport takes place only in the fracture water in the rock, where the mechanisms are diffusion and

convection. Since the diffusing components (the oxidants) have a low concentration, it can be justifiably assumed that concentration changes do not affect the properties of the water (density, viscosity). In this case, the computations for flow and transport of oxidants can be handled separately. The flow field in an individual fracture can be calculated first without any consideration having to be given to the concentration of oxidant. The transport of oxidant in the water with known flow velocities and directions can then be calculated.

2.1.1 Mathematical description

Under steady-state conditions, mass transport in the flowing water in a thin plane fracture can be expressed by the equation:

$$D_v \cdot \left[\frac{1}{r} \frac{\partial}{\partial r} \left(r \frac{\partial c}{\partial r} \right) + \frac{1}{r^2} \cdot \frac{\partial^2 c}{\partial \theta^2} \right] - v_r \cdot \frac{\partial c}{\partial r} - v_\theta \cdot \frac{\partial c}{\partial \theta} = 0 \qquad (2.2)$$

v_r and v_θ are assumed to be known, see 2.1.2.

This is the usual continuity equation for a dissolved component with cylindrical coordinates in two dimensions. The first two terms stand for diffusion in the r and θ directions and the last two for convective transport in the r and θ directions, respectively. In our case, r is the distance from the centre of the canister and θ is the angle from the front of the canister, counting from the direction of impingement (see fig. 2.5). The fracture is considered to be so thin that there is no concentration difference across it.

Boundary conditions

$$c = c_2(\theta) \qquad r = r_2 \qquad 0 < \theta < \pi \tag{2.3}$$

$$c = c_o \qquad r \to \infty \qquad 0 < \theta < \pi \tag{2.4}$$

$$\frac{\partial c}{\partial \theta} = 0 \qquad r \geqslant r_2 \qquad \theta = 0 \tag{2.5}$$

$$\frac{\partial c}{\partial \theta} = 0 \qquad r \geqslant r_2 \qquad \theta = \pi \tag{2.6}$$

Condition 2.3 means that the concentration of the component at the boundary between the fracture and the clay is dependent on the place. This condition gives a coupling to the conditions in the clay in the hole. The concentration in the clay's pore water at the fracture mouth is equal to the concentration in the groundwater at the fracture mouth.

In the computations presented in this report, the conditions in the fracture are first dealt with independently of the conditions in the clay. In this case, c_2 (θ) is set = 0. In the later, complete calculations, the clay and the fracture are dealt with as a continuous medium with varying material properties, and condition 2.3 is automatically fulfilled.

The quantity of oxidants tranported in per unit time is given by:

$$N = -2D_v \cdot r_2 \cdot 2b \int_0^{\pi} \frac{\partial c}{\partial r}\Big|_{r=r_2} d\theta \tag{2.7}$$

(for reasons of symmetry, integration is only carried out over half the cylinder surface).

A mass transfer coefficient is defined by combining equation 2.7 with:

$$N = k_v \cdot 2\pi r_2 \cdot 2b \cdot \Delta c$$

Giving:

$$k_v = - \frac{D_v \cdot \int_0^{\pi} \frac{\partial c}{\partial r}\Big|_{r=r_2} d\theta}{\Delta c} \qquad (2.8)$$

The mass transfer coefficient k_v is a quantity that has been found to be useful in summarizing complex mass transfer cases. It simplifies comparisons between different cases. Many different mass transfer cases are described in the literature (see e.g. Bird, Steward & Lightfoot (4)), and comparisons can therefore be made with other, similar situations. The integral in equation 2.8 is evaluated with the aid of equation 2.2. The latter includes the flow velocities v_r and v_θ . In this treatment, these two velocity components have been assumed to be independent of the distance from the fracture walls, but in reality there is a large difference between the velocity near the wall and the velocity in the centre of the fracture. In actuality, the large friction against the wall is a prerequisite in order for potential flow to prevail. However, the fractures are very thin (<1 mm) and the times are long (>1 year), which means that the concentrations of the dissolved substances have time to even out across the fracture. In the case of diffusion across an aperture, where the concentration in one half of the aperture

is 1 and the concentration in the other half is 0, the concentration evens out to 95% of the equilibrium value (=0.5) after a time $t = b^2/D$ 250 s or slightly more than 4 minutes for small molecules dissolved in water (5). These molecules have diffusivity of $D = 10^{-9}$ m^2/s (6).

The effect on the velocity profile of the clay at the fracture mouth is neglected, due to the fact that the distance to the clay surface is large compared to the distance to the fracture wall for most of the fracture that is of interest (see fig. 2.4). It has been shown in KBS TR 79 as well as in following calculations that the cases that are of interest have a distance of hundreds to thousands of millimetres from the clay in the hole. This is to be compared with the maximum fracture width of 1 mm.

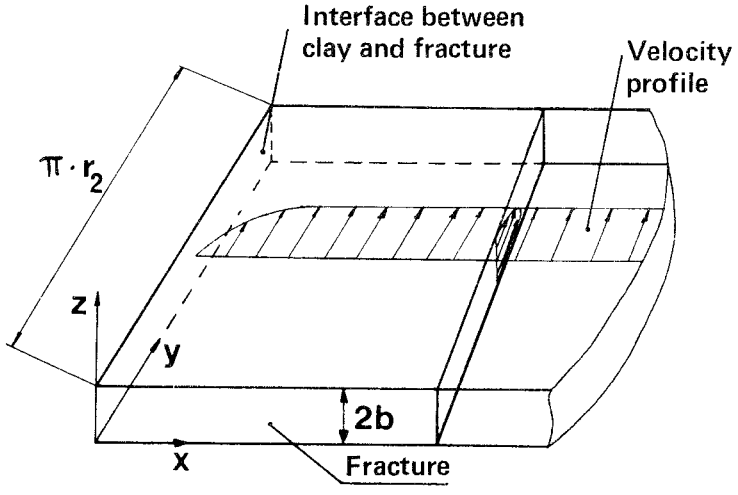

Figure 2.4. Velocity profiles in the flowing groundwater in the fracture.

2.1.2 The flow field

In order to be able to solve equation (2.2), it is necessary to know how the velocity components v_r and v_θ of the flow field are dependent on r and θ. This relationship can be obtained with the aid of potential theory. The following applies for laminar flow between two equidistant plane plates in the s direction:

$$\langle v \rangle = -\frac{b^2}{3\mu}\frac{\partial P}{\partial s} \qquad (2.9)$$

where

P = p + ρgz
z = height above some plane of reference
<v> = the average velocity over the flow cross-section

If the potential $\phi = \frac{P}{\rho g}$ [m] is inserted, the following is obtained if ρ is constant:

$$\langle v \rangle = -\frac{b^2 \rho g}{3\mu}\frac{\partial \phi}{\partial s} \qquad (2.10)$$

The vectorial form of equation (2.10) is obtained through scalar multiplication by s, the unit vector in the s direction

$$\vec{v} = -K\nabla\phi \qquad (2.11)$$

where

$$K = \frac{b^2 \rho g}{3\mu} \quad m/s$$

< > has been removed for the sake of simplicity. The following form of the continuity equation applies for an incompressible fluid:

$$\nabla \cdot \vec{v} = 0 \qquad (2.12)$$

Inserting the expression for $\vec{v}$ (equation (2.11)) in equation (2.12) gives the following if K is a constant:

$$\nabla^2 \phi = 0 \qquad (2.13)$$

This is the Laplace equation.

At this stage, it can be worthwhile to summarize what assumptions have been made in order to obtain equation (2.13)

- constant fracture width 2b
- μ, ρ constant
- laminar flow (low velocities)
- steady-state conditions

It should be noted that equation (2.13) also applies for steady-state flow in a homogeneous, isotropic porous material. Consequently, equation (2.13) is also valid for fractures that can be described in accordance with this equation. This applies, for example, to fractures filled with some permeable "homogeneous" material.

The flow case of interest to us consists of potential flow around a cylinder (fig. 2.5). This case of equation (2.13) has been solved by means of complex analytical methods, and the solution is presented e.g. in Bird et al. ((4) p. 136) for Cartesian coordinates.

For cylindrical coordinates, the velocity components are:

$$v_r = v_\infty \left[-\left(1-\left(\frac{r_2}{r}\right)^2 \cos 2\theta\right) \cos\theta + \left(\frac{r_2}{r}\right)^2 \sin 2\theta \sin\theta \right] \quad (2.14)$$

$$v_\theta = v_\infty \left[\left(1 - \left(\frac{r_2}{r}\right)^2 \cos 2\theta\right) \sin\theta + \left(\frac{r_2}{r}\right)^2 \sin 2\theta \cos\theta \right] \quad (2.15)$$

2.2 Diffusion in the clay

2.2.1 Mathematical description

Diffusion through the clay can also be described by means of the continuity equation for the dissolved component, but here convective transport is negligible, owing to the very low permeability of the clay. Unlike the fracture, which was regarded as a two-dimensional phenomenon, the clay must be regarded as a three-dimensional body.

$$D_L \cdot \left[\frac{1}{r} \cdot \frac{\partial}{\partial r}\left(r \frac{\partial c}{\partial r}\right) + \frac{\partial^2 c}{\partial z^2} + \frac{1}{r^2} \cdot \frac{\partial^2 c}{\partial \theta^2} \right] = 0 \quad (2.16)$$

Since steady-state conditions prevail, the possible sorption of oxidants by the clay does not have to be taken into consideration.

The terms stand for diffusion in the r, z and θ direction. The boundary conditions are

$$c = 0 \qquad r = r_1 \qquad 0 < z < \frac{s}{2} \qquad \text{alla } \theta \quad (2.17)$$

$$c = c_2(\theta) \qquad r = r_2 \qquad 0 < z < b \tag{2.18}$$

$$\frac{\partial c}{\partial r} = 0 \qquad r = r_2 \qquad b \leq z \leq \frac{s}{2} \qquad \text{alla } \theta \tag{2.19}$$

$$\frac{\partial c}{\partial z} = 0 \qquad r_1 < r < r_2 \qquad z = \frac{s}{2} \qquad \text{alla } \theta \tag{2.20}$$

$$\frac{\partial c}{\partial z} = 0 \qquad r_1 < r < r_2 \qquad z = 0 \qquad \text{alla } \theta \tag{2.21}$$

$$\frac{\partial c}{\partial \theta} = 0 \qquad r_1 < r < r_2 \qquad 0 < z < \frac{s}{2} \qquad \theta=0 \text{ och } \theta=\pi \tag{2.22}$$

The oxidant flow in from the water is obtained by:

$$N = 2r_2 \cdot D_L \cdot 2b \cdot \int_0^{\pi} \frac{\partial c}{\partial r}\Big|_{r=r_2} \cdot d\theta \tag{2.23}$$

Condition 2.17 means that the oxidant reacts immediately with the canister material and 2.18 defines the conditions in the interface between the water in the fracture and the clay. When considering the conditions in the clay alone, $c_2(\theta)$ is set = c_o for all θ. Condition 2.19 says that the rock does not absorb or give off oxidant. Conditions 2.20-2.22 are expressions for the symmetry of the system.

2.3 Transport through the continuous clay - fracture system

A calculation has also been carried out for the continuous clay-fracture system. This process is described by the same

equations as before, with the exception of boundary conditions (2.3) and (2.18). These conditions are replaced with a mass flow condition between the water in the fracture and the clay. The result is nevertheless that the concentrations in the liquid are equal. A variable concentration is then obtained along the interface between the clay and the fracture.

2.4 Numerical solution

The model equations have been solved numerically with the aid of a computer program (TRUMP) developed at Lawrence Livermore Laboratories in the United States (7). The numerical method that it used (the integrated finite difference method) is based on the fact that the three-dimensional space is divided into a number of volume elements, the size and form of which can be chosen fairly freely. A point (node) is designated in each such volume element in which the properties of the element are assumed to be situated.

The basic idea of the program is very simple. An element can give off or obtain mass (or energy) through exchange with nearby elements. The exchange can take place by the mass being transported over the interface between the elements through diffusion and/or through flow. Each element can be enriched (depleted) of the substance through accumulation and through chemical reaction. Conditions at a later point in time can be calculated from known conditions by systematically calculating the mass transport into and out of each element from prevailing conditions in the element and its neighbours by keeping a record of everything that enters, leaves, accumulates or reacts.

This approach eliminates the necessity of formulating the previously described partial differential equations 2.2 and 2.16. The formulation described above can be done directly. If equations 2.2 and 2.16 are used, a discretizing of space is necessary for the numerical treatment which leads to the same treatment of elements as is described above.

In practice, the integrated finite difference method as it is formulated in the program allows very great flexibility in the choice of size and shape of the elements. Time stepping is done with modern implicit methods or by the use of a direct solution method for the resulting matrix. A detailed description of the numerical method is presented in (8).

In practice, the program is used as follows.

Physical data are entered for each node. The data can vary between the nodes. The volume of each node as well as its interface with nearby nodes are specified. In the next step, the nodes that are connected with each other are specified. The program then calculates the mass exchange, diffusive and/or convective, between the coupled nodes. This procedure eliminates the necessity of specifying the dimension of the problem. When time-independent problems are solved, the problem is solved as if it were time-dependent, but the demand on accuracy during the time-dependent phase is set low.

2.4.1 Discretizing

The accuracy of all numerical solutions is dependent on how time and space are divided. The best division varies from

problem to problem, depending on its nature. An attempt is made to make the increments small in those directions where the gradients are large. It is particularly important in the clay diffusion case to have a very fine graduation near the fracture, since the concentration profile here is very steep. This is associated with the fact that the diffusion area at the transition from the fracture to the clay barrier instantaneously increases by a factor of about 1000-10000. This means that the concentration drops very rapidly.

Furthermore, in order to keep the number of nodes down, an attempt is made to utilize symmetry as far as is possible. In the film resistance case, this has been done by only taking into account half the circumference at the interface between the groundwater and the fracture. See fig. 2.5.

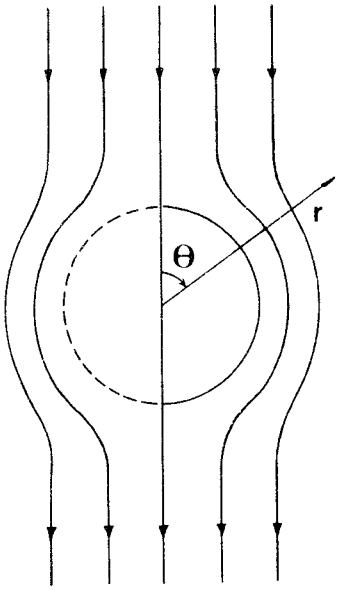

Figure 2.5 Groundwater flow around the canister.

The number of nodes and their lengths in the different coordinate directions have been chosen by first making an estimate of the expected concentration profiles. Small and relatively many nodes have been located in areas where a steep profile is expected. The node sizes, and in some cases the number of nodes as well, have then been systematically varied in order to ascertain how this affects the results.

In calculating the resistance in the fracture, 6, 12 and 24 intervals were used in the θ direction on half the circumference and 28 in the r direction. The length of the first node (nearest the clay barrier) was 1.3 mm and the length of the following 13 was increased successively by a factor of 1.733, i.e. the length Δr_n of node n is obtained as: $\Delta r_n = \Delta r_1 \cdot q^{n-1}$, where q is the geometric factor. A factor of 2.0 was used for the remaining nodes. The variation in the quantity of oxidants transported in when 6 versus 24 intervals in the θ direction were used was less than 3%. Similar results were obtained when the increments in the r direction were varied.

The calculations of diffusion in the clay barrier for a fracture width of 0.1 mm were very difficult to carry out, on the other hand, owing to numerical problems. These problems stem from the fact that it is necessary to use nodes with very large differences in volume in the numerical solution. Ratios between the volumes of the largest and smallest nodes of 10^8 may be necessary sometimes. In the beginning of the clay barrier (nearest the fracture mouth), where the concentration profile is very steep, small nodes are required for reasons of accuracy. At the end, where the profile is not so steep, larger nodes can be used. But in

this special case, larger nodes must be used, since the total number of nodes would otherwise be so large that there would not be room for them in the computer's memory. The difference in size between the largest and smallest nodes is therefore sometimes far too great, for the smallest fracture studied, 0.1 mm.

In order to get around this problem, the calculations have instead been carried out for a 1 mm fracture. A less steep concentration profile is thereby obtained than with a 0.1 mm fracture, which means that larger nodes can be used. An idea of how large an error is thereby introduced can be obtained by applying the equation that was used in KBS TR 79 to describe diffusion from the fracture to the canister. This diffusion was assumed there to take place between two concentric cylinders. The inner cylinder corresponds to the fracture and the outer to the canister. Mass transport between the cylinders is given by equation (2.24), where δ is put equal to s. In the equation, it is seen that the mass transport is inversely proportional to the logarithm of the radius ratio r_2/r_1. In this case, r_2 corresponds to the fracture spacing s and r_1 to the fracture width 2b, i.e.:

$$N = \frac{\text{const}}{\ln \frac{s}{2b}}$$

If s = 1 m and 2b = 10^{-4} and 10^{-3} m, respectively, are now inserted, the ratio between inward transport in the two places is obtained as:

$$\frac{N''}{N'} = \frac{\ln 10^3}{\ln 10^4} = \frac{3}{4}$$

In other words, the inward transport is about 25% higher for the 1 mm fracture and for the 0.1 fracture.

It is evident from the above that the reduction of the mass flow in the clay in connection with a reduction in the fracture width is small and estimable. For this reason, and the fact that the resistance of the clay is small compared to the transport resistance in the water in the fracture, the program is not refined to be able to calculate for the finest fractures. The number of intervals in the clay barrier in the r direction was 35 and in the z direction 15. The first node (nearest the fracture mouth) was $5 \cdot 10^{-4}$ m in the r direction and was increased successively by a factor of 1.12. In the z direction, the first node (nearest the fracture) was 10^{-4} m and the factor was 1.72. The number of intervals in the θ direction was 6.

2.5 Comparison with equations used in KBS TR 79

The transport of oxidants into the canister was previously dealt with in KBS TR 79. The geometry was simplified there so that the steady-state mass transport can be described by means of one-dimensional relationships. What has been done is the following: The cylindrical diffusion symmetry in the clay barrier has been transferred to a plane geometry by using an average diffusion area that can be calculated with the aid of the logarithmic average radius r_m. See figs. 2.6 and 2.7.

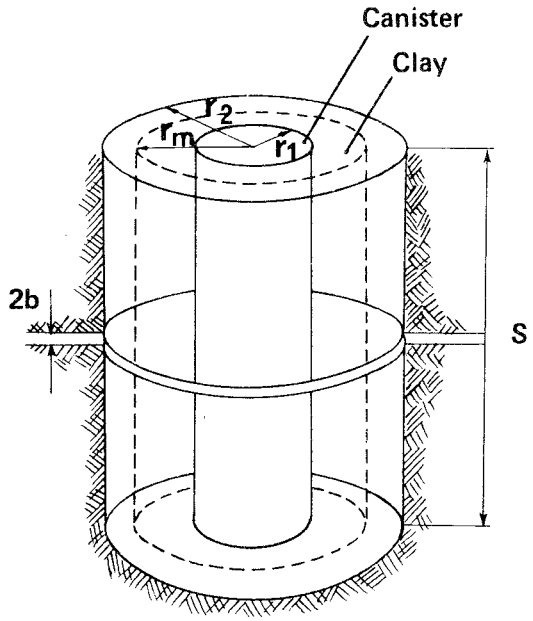

Figure 2.6

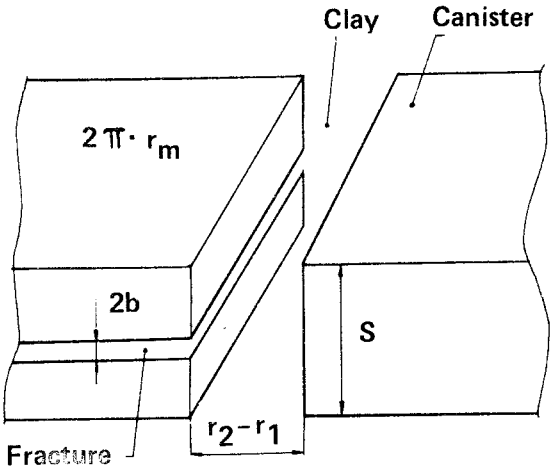

Figure 2.7

The problem has now been shifted to diffusion between two plane-parallel plates with a length of $2\pi \cdot r_m$. The diffusion is still two-dimensional, however, since the area at the fracture mouth is instantaneously changed from the fracture width to the fracture spacing. The next step is therefore to approximate it with a one-dimensional diffusion. This has been done by regarding it as diffusion between two concentric cylinders, where the radius of the inner cylinder consists of half the fracture width and the radius of the outer cylinder consists of half the fracture spacing. See fig. 2.8. With this procedure, an average diffusion area can once again be defined by introducing δ ($= \frac{s-2b}{\ln \frac{s}{2b}}$). See fig. 2.9.

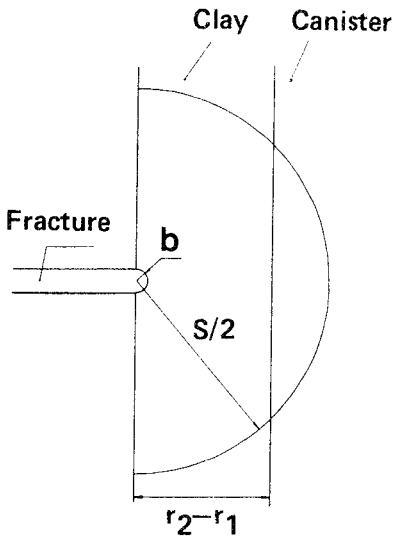

Figure 2.8

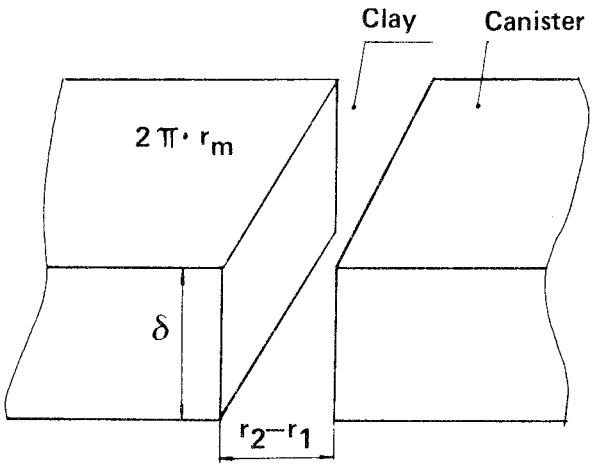

Figure 2.9

With these two approximations, the mass transport in the clay barrier for a single fracture is obtained by:

$$N = \delta \cdot 2\pi \cdot r_m \cdot D_L \cdot \frac{\Delta c_L}{r_2-r_1} \qquad (2.24)$$

where $r_m = \dfrac{r_2-r_1}{\ln\frac{r_2}{r_1}}$

The above simple relationships can be regarded as an approximation to equation (2.23). A coupled flow and mass transport is obtained at the interface between the groundwater and the clay barrier. When the groundwater sweeps past, the dissolved oxidants simultaneously diffuse into the clay. Transport by means of this mechanism can be expressed by means of a relationship analagous to equation (2.24) where $\dfrac{D_L}{r_2-r_1}$ is

replaced by a constant, k_v. This constant is usually called the mass transfer coefficient and is written as

$$k_v = \sqrt{\frac{4 \cdot D_v}{\pi \cdot t_k}} \qquad (2.25)$$

The contact time t_k $(= \frac{\pi \cdot r_2}{u_p})$ is defined as the time a "liquid parcel" with a velocity of u_p remains at the interface. D_v is its diffusivity in the water. The equation for a <u>singe</u> fracture is then:

$$N = 2b \cdot 2\pi \cdot r_2 \cdot k_v \cdot \Delta c_v \qquad (2.26)$$

This applies strictly under the provision that:

- The liquid flow is laminar
- The concentrations are low
- Diffusion in the flow direction of the water is neglected
- The interface is plane
- The canister is regarded as infinitely long
- The influence of other canisters is neglected
- Small depth of penetration

With the above assumptions, the mass transfer coefficient can be derived by applying the diffusion equation to a volume element that moves along the interface. The process can namely be regarded as a non-steady-state diffusion process in the water, where the diffusion time consists of

the contact time ((4) p. 539). In this way, the mass transport between the water, the fracture and the clay can be obtained with the aid of:

$$D_v \frac{\partial^2 c}{\partial x^2} = \frac{\partial c}{\partial t} \qquad (2.27)$$

where x is the distance out into the water from the clay surface.

with the following boundary and initial conditions

$c = 0$	$x = 0$	$t > 0$
$c = c$	$x \rightarrow \infty$	all t
$c = c_o$	all x	$t = 0$

The solution to equation (2.27) gives the concentration as a function of the location (x) and the time (t):

$$c = c_o \cdot \text{erf}\ (x/\sqrt{4D_v \cdot t}) \qquad (2.28)$$

The mass flow is obtained by integrating the flow at the phase interface over the contact area:

$$N = 2 \cdot \int_o^{t_k} \int_o^{2b} - D_v \cdot \frac{\partial c}{\partial x}\Big|_{x=0} \cdot dz \cdot dt \qquad (2.29)$$

The following is then obtained:

$$N = 2b \cdot 2\pi \cdot r_2 \sqrt{\frac{4D_v}{\pi \cdot t_k}} \cdot c_o \qquad (2.30)$$

which agrees with equations 2.25 and 2.26.

2.6 Results

In the first part of the calculations, the two transport resistances (R_L and R_v) are separated, i.e. when the one resistance is calculated, the influence of the other is neglected. By utilizing the general equation for steady-state mass transport, a ficticious mass transport coefficient can then be defined for the clay. In this coefficient, the influence of fracture width, fracture spacing and diffusivity are lumped together. The following is then obtained:

$$N = k_L \cdot A_L \cdot \Delta c_L \qquad (2.31)$$

A_L is the area through which diffusion takes place. In this case, it is chosen as the contact area between the clay and the rock. In the same way, the following is obtained between the groundwater and the clay:

$$N = k_v \cdot A_v \cdot \Delta c_v \qquad (2.32)$$

A_v is the fracture's contact area against the clay. A total mass transfer coefficient, K, can now be defined by making use of the fact that the total concentration difference c is given by:

$$\Delta c = \Delta c_L + \Delta c_v \qquad (2.33)$$

The following is then obtained:

$$N = K \cdot A \cdot \Delta c \qquad (2.34)$$

Where $$K = \frac{1}{\frac{A}{k_L \cdot A_L} + \frac{A}{k_v \cdot A_v}} \qquad (2.35)$$

If A_L is chosen as the reference area ($A = A_L$), the following is obtained:

$$\frac{1}{K \cdot A_L} = \frac{1}{k_L \cdot A_L} + \frac{1}{k_v \cdot A_v} \qquad (2.36)$$

The expression (2.36) means that the individual resistances can be added in order to obtain the total resistance, since $1/KA = R$ in accordance with a former definition.

$$R_{TOT} = R_L + R_v$$

It is evident from equation 2.34 that the area for the transport is of crucial importance. Since the clay's area for diffusion, which in this case is equal to its contact area against the rock, is considerably greater than the fracture mouth's area against the clay (A_v), R_v can be expected for this reason alone to be large in relation to R_L when the fracture width is small.

Values of $k_L \cdot A_L$, $k_v \cdot A_v$ and $K \cdot A_L$ for the fracture widths 0.1 and 1 mm are found in table 2.1. They have been calculated using both the simple relationships obtained in KBS TR 79 and the more complex relationships presented in sections 2.1 and 2.2. The latter were obtained with the computer program TRUMP (7).

The following values of the parameters have been used:

$D_L = 7.8 \cdot 10^{-11}$ m^2/s, $D_v = 3.9 \cdot 10^{-9}$ m^2/s

$S = 1$ m, $u_o = 3.15 \cdot 10^{-4}$ m/year

$r_1 = 0.375$ m, $r_2 = 0.75$ m

Table 2.1 Product of mass transfer coefficient and transport area

Fracture width	$k_L \cdot A_L \times 10^3$		$k_v \cdot A_v \times 10^3$	
(mm)	KBS TR 79	TRUMP	KBS TR 79	TRUMP
0.1	4.8		0.22	0.24
1.0	6.5	6.0	0.68	0.78

The resistances in the two barriers for the different cases are presented in table 2.2. It is seen there that the resistance in the clay has very little influence on the total resistance.

Table 2.2 Resistance for one fracture

Fracture width	$R_L \times 10^{-3}$		$R_v \times 10^{-3}$		$R_{TOT} \times 10^{-3}$	
(mm)	KBS TR 79	TRUMP	KBS TR 79	TRUMP	KBS TR 79	TRUMP
0.1	0.21		4.6	4.2	4.8	4.4
1.0	0.15	0.17	1.5	1.3	1.6	1.5

The total resistance for the continuous clay-fracture system, i.e. when equations 2.2 and 2.16 are coupled together, is given in table 2.3

Table 2.3 Resistance for one fracture calculated with TRUMP (continuous system)[++)]

Fracture width[+)] (mm)	$R_L \times 10^{-3}$	$R_V \times 10^{-3}$	$R_{TOT} \times 10^{-3}$
1	0.2	1.4	1.6

+) Unfortunately, the calculations could not be carried out with the smaller fracture width (0.1 mm) owing to the numerical problems mentioned earlier. (Too large a span in node size.)

++) The calculated resistance is an average value around the cylinder surface. These results can be compared directly with those in table 2.2.

3. RADIOLYSIS

When atomic radiation is absorbed in water, the water decomposes according to the following schematic formula:

$$aH_2O \xrightarrow{+h\nu} be^-_{(aq)} + cOH^{\cdot} + dH^{\cdot} + fH_2 + gH_2O_2$$

In pure irradiated water, there is no net decomposition due to the reverse reactions:

$$H_2 + OH^{\cdot} \longrightarrow H_2O + H^{\cdot}$$

$$H_2O_2 + H^{\cdot} \rightarrow H_2O + OH^{\cdot}$$

$$H_2O_2 + e^-_{(aq)} \rightarrow OH^- + OH^{\cdot}$$

A net decomposition can only take place if the water contains impurities that can react with the radicals $H^{\cdot}$, $OH^{\cdot}$ and $e^-_{(aq)}$ so that the above reverse reactions are prevented.

The substances which are of interest in our case are hydrogen (H_2) and hydrogen peroxide (H_2O_2). Both of these affect conditions in the canister's immediate surroundings. Due to its oxidizing capacity, hydrogen peroxide can change the environment in the repository from reducing to oxidizing. The solubility of many radionuclides is considerably higher in an oxidizing environment (20). In the event of a cansiter leak, this means that larger concentration gradients are created for these radionuclides, which in turn means a higher outward transport rate. The redox potential affects not only solubility, but also sorbency. For many actinides, sorbency is lower under oxidizing conditions.

The second problem is the hydrogen. If the hydrogen gas cannot migrate out through the clay, it is not inconceivable that considerable hydrogen gas pressures might build up inside the clay barrier. In the extreme case, the pressure could become so high that movements occur in the surrounding rock. In this manner, fractures can be widened, resulting in a higher water flow around the repository.

The calculations presented below are approximations for the purpose of illustrating which transport mechanisms are of importance. At this stage, it is not meaningful to carry out detailed calculations, since the magnitude of many important parameters is subject to great uncertainty.

The radiolysis is mainly caused by α-radiation and γ-radiation. These two types of radiation differ with respect to their range. γ-radiation has the longest range. Its half-value thickness in copper is about 1 cm or less, depending on the energy of the radiation. The effects of γ-radiation can be reduced to the desired level by means of shielding. In order for α-radiolysis to occur, the canister must be damaged so that water comes into direct contact with the radioactive waste. The range of α-radiation in water is about 0.03 mm (11). This short range means that the magnitude of the radiolysis is directly proportional to the exposed surface area.
Dissolution of the waste into smaller particles therefore leads to considerably higher radiolysis if more water penetrates at the same time.

The production rates of hydrogen and hydrogen peroxide in connection with α-radiolysis on which the calculations in this report are based have been obtained by assuming that the total cylindrical surface of the fuel pellets in 499 rods is in direct contact with water. The radiochemical calculations were carried out by Christensen et al. (19). The results of these calculations are presented in the tables below in the form of cumulative hydrogen quantities at certain points in time and production rates.

Table 3.1 Hydrogen production as a result of radiolysis for canister thicknesses 1, 6 and 20 cm (BWR 33) (from Christensen et al. (10))

	Integrated production (moles)			Production rate (moles/year)		
Canister thickness (cm)	1	6	20	1	6	20
Time (years)						
10^2	1	1	$2 \cdot 10^{-3}$	$8 \cdot 10^{-3}$	$8 \cdot 10^{-3}$	$2 \cdot 10^{-5}$
- 10^5	47	3	$7 \cdot 10^{-2}$	$4 \cdot 10^{-4}$	$2 \cdot 10^{-6}$	$0.6 \cdot 10^{-6}$
10^6	390	32	0.6	$4 \cdot 10^{-4}$	$3 \cdot 10^{-6}$	$0.6 \cdot 10^{-6}$

Table 3.2 Hydrogen production as a result of radiolysis, based on the cylindrical surface area of the fuel pellets in 499 rods of spent fuel (from Christensen et al. (11)).

Time	Integrated production (moles)	Production rate (mole/year)
10^2	540	2.4
10^5	13 070	0.013
10^6	22 000	0.005

3.1 Outward transport of hydrogen

The water is now assumed to be radiolysed. Hydrogen is formed in the quantities given in tables 3.1 and 3.2 for the two different types of radiation and at the different times. It is assumed that the inward transport of water in sufficient quantity to sustain the radiolysis does not constitute a limiting factor. The mechanisms that are available for transporting hydrogen away are diffusion and displacement.

3.1.1 Diffusion

Since the pores in the clay and the rock are filled with water, the hydrogen must first dissolve in the water before it can diffuse away. The driving force for diffusion is determined by the solubility of hydrogen in water. This solubility is pressure-dependent and is assumed to follow Henry's law, i.e. it is directly proportional to the hydrogen pressure. For moderate pressures (<10 bar), this is given by (9, p. 3-97):

$$x_1 = \frac{P}{6.83 \cdot 10^4} \quad \text{(P in bar)} \tag{3.1}$$

To simplify the calculation, the canister is approximated by a sphere with a radius of r_1, and the region around it is regarded as infinite. If the diffusivity is assumed to be equal in the water-filled pores in both the rock and the clay, and if the concentrations are low (12, 13), the mass transport under steady-state conditions can be described by:

$$N = - D_{eff} \cdot 4\pi \cdot r^2 \cdot C_{TOT} \cdot \frac{dx}{dr} \tag{3.2}$$

which is integrated as follows:

$$\int_{x_1}^{x} dx = \frac{-N}{4\pi \cdot D_{eff} \cdot C_{TOT}} \int_{r_1}^{r} \frac{dr}{r^2} \tag{3.3}$$

to

$$x - x_1 = \frac{-N}{4\pi \cdot D_{eff} \cdot C_{TOT}} \left(- \frac{1}{r} + \frac{1}{r_1}\right) \tag{3.4}$$

At infinite distance, $x = 0$ and $\frac{1}{r} \rightarrow 0$, which gives

$$N = 4\pi \cdot r_1 \cdot D_{eff} \cdot C_{TOT} \cdot x_1 \tag{3.5}$$

In equation (3.5), the mole fraction x_1 is included as the driving force. If this is now combined with equation (3.1), the following is obtained:

$$P = \frac{6.83 \cdot 10^4 \cdot N}{4\pi \cdot r_1 \cdot C_{TOT} \cdot D_{eff}} \quad \text{(bar)} \qquad (3.6)$$

The hydrogen pressures required to transport away the hydrogen that is formed are tabulated below. The following data have been used in the calculations:

r_1 = 1 m, D_{eff} = 2.10^{-11} m^2/s (see reference (12))
C_{TOT} = 55.6 $kmol/m^3$

Table 3.3 Hydrogen pressure required for the hydrogen that is formed to be transported away by diffusion under quasi-steady-state conditions (γ-radiolysis).

Time (years)	Hydrogen pressure (bar)		
	Canister thickness (cm)		
	1	6	20
10^2	1.3	1.3	$3.2 \cdot 10^{-3}$
10^5	0.065	$5 \cdot 10^{-4}$	$1 \cdot 10^{-4}$
10^6	0.065	$5 \cdot 10^{-4}$	$1 \cdot 10^{-4}$

Table 3.4 Hydrogen pressure required for the hydrogen that is formed to be transported away by diffusion under quasi-steady-state conditions (α-radiolysis).

Time (years)	Hydrogen pressure (bar)
10^2	372
10^5	2
10^6	0.8

Conclusion

Table 3.3 shows that the hydrogen formed as a result of γ-radiolysis can easily diffuse away. The highest required hydrogen pressure is only 1.3 bar. The situation is somewhat different for the α-radiolysis. There, hydrogen is produced at 100 years in such quantities that a hydrogen pressure of 390 bar would be required under steady-state conditions for the outward transport. The probability of this happening, i.e. the probability of a canister being damaged after 100 years to the extent that water enters and wets all the fuel pellets, would appear to be low. It will be shown below that displacement of the water in the pores in the clay can take place at lower pressures and the hydrogen can therefore flow out instead.

3.1.2 Displacement

Highly compacted bentonite clay has very low permeability (13). The flow of water in its pores will therefore be completely negligible at the prevailing natural hydraulic gradient. It would otherwise be possible for the hydrogen to dissolve in the pore water, which would then flow away. Since this is not possible, the only remaining mechanism is displacement, i.e. the built-up hydrogen pressure displaces the water in the clay. Since the actual process is very complicated, simplifications must be introduced:

- The calculations are only carried out for clay, since clay is assumed to have a much lower permeability than rock. The water flow in the clay therefore determines what pressure drop is required.

- The displacement is assumed to take place in a radial direction along the entire length of the canister with a plane interface between gas-filled and water-filled pores (see fig. 3.1).

- A prerequisite for displacement to take place along the entire surface of the canister is that the hydrogen pressure should exceed the hydrostatic pressure at the lowest point in the repository. With the repository 500 m below the surface and a canister length of 5 m, this pressure is 50.5 bar (see fig. 3.1).

- The flow cross-section available for the transport is based on the canister's surface area.

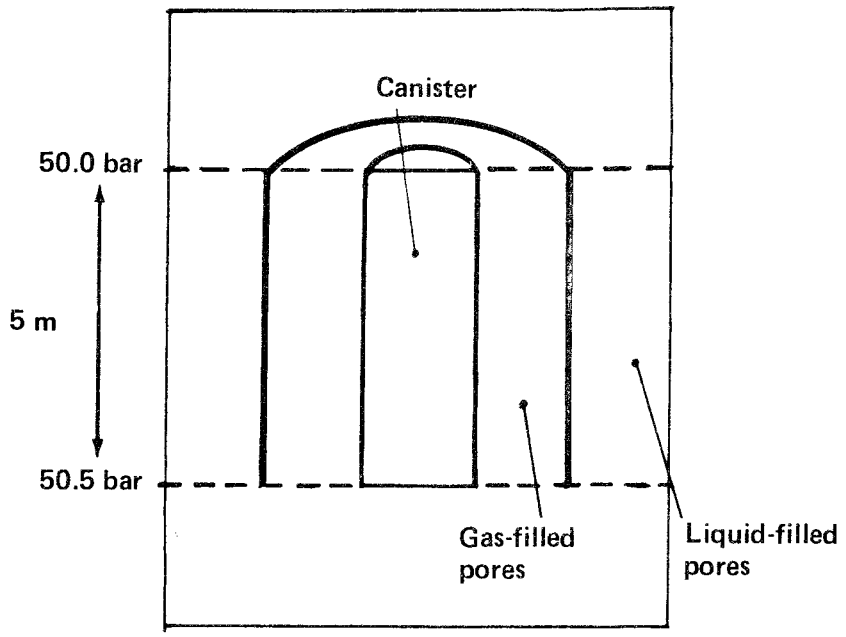

Figure 3.1 Displacement of the pore water in the buffer material

With the above assumptions, the displacement can be calculated using Darcy's equation and the gas law:

$$\frac{\dot{n}RT}{\Delta p + p_o} = \frac{A \cdot K_p \cdot \Delta p}{\rho_{H_2O} \cdot g \cdot L} \qquad (3.7)$$

The left-hand side is the hydrogen gas volume produced per unit time at the prevailing pressure, $\Delta p + p_o$, and the right-hand side includes material constants and the driving force, which determine the transport rate. If the equation is solved for Δp the following is obtained:

$$\Delta p = -\frac{p_o}{2} + \sqrt{\frac{\dot{n}RT\rho_{H_2O} \cdot g \cdot (r_2 - r_1)}{A \cdot K_p} + \left(\frac{p_o}{2}\right)^2} \qquad (3.8)$$

Data used

$A = 10\ m^2$
$K_p = 10^{-14}$ m/s for water
$T = 298$ K
$p_o = 50$ bar
$r_2 - r_1 = 0.4$ m

Tables 3.5 and 3.6 present the pressures required to displace the pore water in the clay.

Table 3.5 Hydrogen pressure required to displace the water in the clay (γ-radiolysis).

Time (years)	Hydrogen pressure (bar) Canister thickness (cm)		
	1	6	20
10^2	$4.9 \cdot 10^{-2}$	$4.9 \cdot 10^{-2}$	$1.25 \cdot 10^{-4}$
10^5	$2.5 \cdot 10^{-3}$	$2 \cdot 10^{-5}$	$5 \cdot 10^{-6}$
10^6	$2.5 \cdot 10^{-3}$	$2 \cdot 10^{-5}$	$5 \cdot 10^{-6}$

Table 3.6 Hydrogen pressure required to displace the water in the clay (α-radiolysis).

Time (years)	Hydrogen pressure (bar)
10^2	12
10^5	$8 \cdot 10^{-2}$
10^6	$3 \cdot 10^{-2}$

3.2 Inward transport of water

In the calculations of hydrogen transport, it is assumed that the supply of water does not constitute a limiting factor. Water can be continuously transported into the fuel pellets at the same rate as it is consumed by radiolysis. Some mechanisms for this water transport are studied in the following calculations.

A hole is assumed to have been made in the canister wall. As a reference case, we have chosen an area of 1 dm^2. The hole is filled with corrosion products (porosity 0.1). It is assumed that the hydrogen does not influence the water transport. The two transport mechanisms for the water through the hole that are dealt with here are water vapour diffusion and capillary flow.

3.2.1 Water vapour diffusion

Water evaporates from the clay surface next to the canister wall and diffuses in the form of vapour through the hole. The driving force for the diffusion consists of the difference

in water vapour pressure between the saturated clay surface and the interior of the canister. If the water vapour pressure in the interior of the canister is set equal to 0, the driving force for diffusion is determined by the saturation pressure at the prevailing temperature (30°C). See figure 3.2.

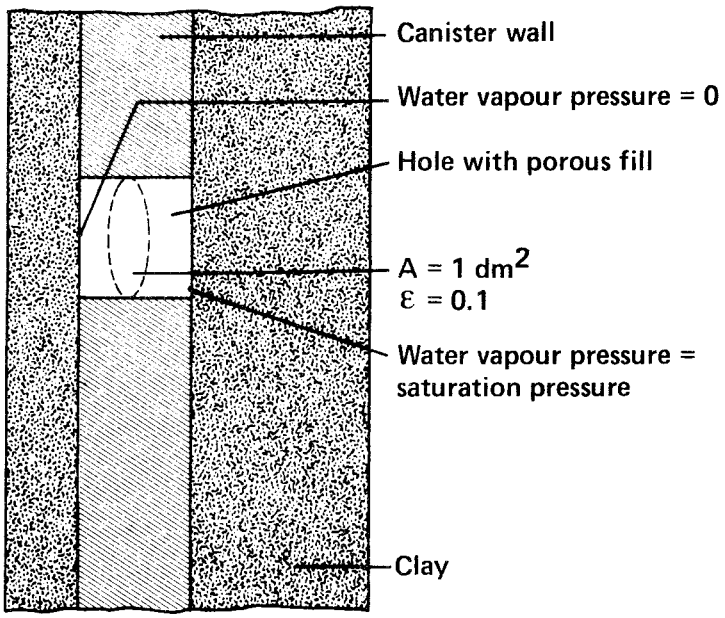

Figure 3.2 Water vapour diffusion through a hole in the canister.

Under the above conditions, the water transport can be calculated by:

$$N = - \frac{A \cdot D_{eff}}{RT} \cdot \frac{\Delta P_{H_2O}}{\Delta Z} \qquad (3.9)$$

Equation (3.9) gives the result that 6.4 moles of water can be transported in per year. The following data have been used in the calculation:

$A = 0.01\ m^2$, $\varepsilon = 0.1$

$\tau^2 = 3$, $D_v = 2.2 \cdot 10^{-5}\ m^2/s$ (see reference (9))

$\Delta P_{H_2O} = 4.2$ kPa (9), $T = 303$ K

$R = 8.314$ J/mol, K, $\Delta Z = 0.06$ m

$$D_{eff} = \frac{\varepsilon \cdot D_v}{\tau^2}$$

Conclusion

The calculated transport rate is of the same order of magnitude as the highest radiolysis rates, which should indicate that the inward transport of water by means of diffusion in the vapour phase does not limit the radiolysis. But one factor that severely limits this transport mechanism, if it is possible at all, is the temperature gradient. It is assumed that water evaporates from the clay surface outside the canister only to condense inside. The temperature inside the canister is higher than the surrounding temperature, which means that the water must condense at a higher temperature than that at which it evaporates. This would appear to be improbable. Radiolysis could then possibly take place in the vapour. No calculations of α-radiolysis in the vapour phase are available for this case. As an initial postulate for short radiation distances (thickness of gas or liquid film), it can be assumed that radiolysis is proportional to water content. At 70°C, the density of saturated water vapour is 0.2 kg/m^3, i.e. about 5 000 times lower than the density of liquid water. Radiolysis is therefore accordingly less.

3.2.2 Capillary flow

Capillary flow is the other possible mechanism by means of which water can be transported into the fuel pellets. The driving force is assumed to arise in the pores of the corrosion product and consist of a capillary pressure. Due to this pressure, water is sucked from the clay into the canister. The flow in the clay is assumed for the sake of simplicity to take place in an imaginary channel with the same cross-sectional area as the hole in the canister (see fig. 3.3). In actuality, water flows from all directions towards the hole, but this is not meaningful in the context of these approximations.

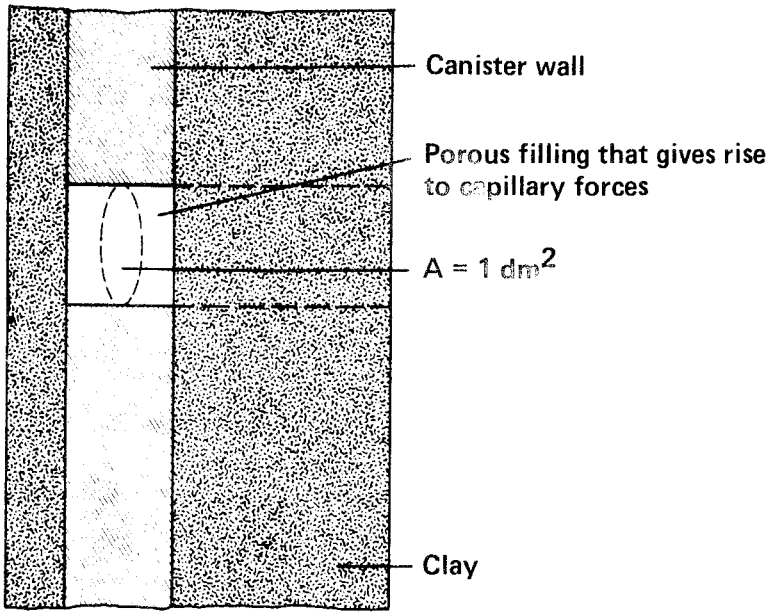

Figure 3.3 Water transport through a hole in the canister wall

Additional simplifications have been made by approximating the system of pores in the corrosion product as pores that are straight, parallel and cylindrical in cross-section. If the contact angle between the liquid and the pore surface is assumed to be 0, the following is obtained:

$$\Delta P_{KAP} = \frac{2 \cdot \sigma}{r_{KAP}} \qquad (3.10)$$

The pressure drop connected with the water's flow in the clay is obtained with Darcy's equation:

$$\Delta P_s = \frac{Q \cdot \rho \cdot g \cdot (r_2 - r_1)}{A \cdot K_p} \qquad (3.11)$$

If the capillary pressure (ΔP_{KAP}) is now set equal to the pressure drop (ΔP_s), which means that the hydrogen does not build up any pressure, the required capillary radius in order for as much water to be transported in as is consumed by the α-radiolysis can be calculated.

$$r_{KAP} = A \cdot K_p \cdot \frac{2 \cdot \sigma}{Q \cdot \rho \cdot g \cdot (r_2 - r_1)} \qquad (3.12)$$

The capillary radii are tabulated in the table below.

Table 3.7 Capillary radii required to keep the α-radiolysis supplied with water

Time (years)	Capillary radius (mm)
10^2	3
10^5	50
10^6	1300

The calculated capillary radii in table 3.7 are based on the following data:

$A = 0.01\ m^2$, $K_p = 10^{-14}$ m/s (see reference (13))
$\varepsilon = 0.1$, $\sigma = 0.073$ N/m
$\rho = 1000\ kg/m^3$, $g = 9.81\ m/s^2$
$r_2 - r_1 = 0.4$ m

Conclusion

The very low hydraulic conductivity (13) that is claimed for highly compacted bentonite clay constitutes a limitation on how much water can be transported in by means of capillary flow. The capillary radius that is required to balance water consumption at 10^2 years is unreasonably small. In addition, the possibility that the corrosion products will have pore radii of 50 nm cannot be ruled out.

3.3 Simultaneous transport of water and hydrogen through a hole in the canister wall

Thus far, the transports of water to and hydrogen away from the waste canisters have been dealt with separately in the approximate calculations. This is not correct, since the hydrogen pressure that is built up inside the canister reduces the inward transport of water by reducing the pressure difference that gives rise to the driving force. When equilibrium has been reached, hydrogen production and inward water transport balance at a lower level than is obtained in the preceding calculations. In these calculations, it is assumed that the hole in the canister wall is filled with

the porous corrosion product with a continuous pore system. Through this pore system, water is sucked from the surrounding clay by the capillary forces that arise in the tiny pores in the corrosion product. The water is radiolysed and hydrogen is formed. This hydrogen flows out in pores that are considerably larger than those that transport the water in. The transport resistance consists of the clay for both the water and the hydrogen, due to the very low hydraulic conductivity of the clay. 50% of the area of the hole is assumed to consist of pores that are sufficiently small to be able to transport water in by means of capillary forces. The pores in the rest of the area of the hole are so large that no real capillary force is created. It is further assumed that the pores are straight, parallel and have a circular cross-section.

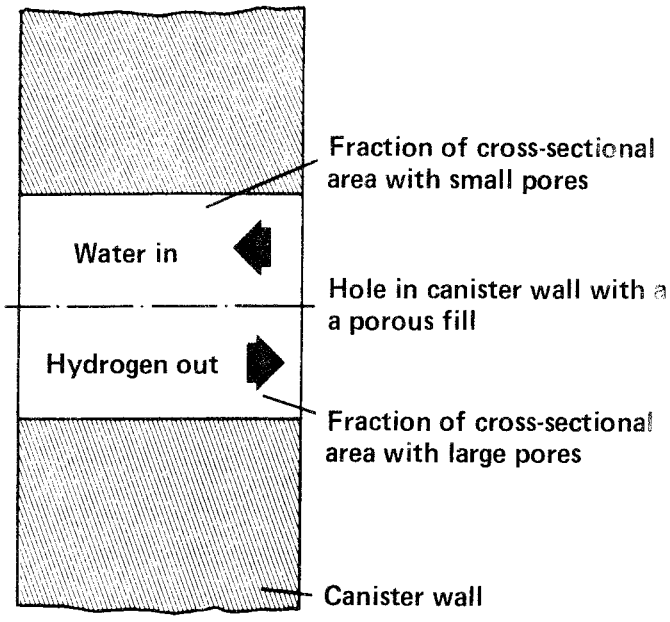

Figure 3.4 Schematic diagram of simultaneous water and hydrogen transport through a porous corrosion product

Equations

The transport of hydrogen and water in the buffer is described by

$$N = K_p \cdot A \frac{1}{\rho g} \frac{dP}{dr} \qquad (3.13)$$

If we imagine that the corrosion product has expanded and forms a hemisphere outside of the hole*, transport to (from) the surface of the hemisphere can be calculated. It is thereby assumed that the buffer has a much larger extent than the diameter of the hole. It is assumed for practical purposes to be infinite. Integrating the pressure from the surface of the sphere ($r = r_o$) to ∞ then gives ($A = 2\pi \cdot r^2$, increasing area with distance)

$$N = 2\pi \cdot r_o^2 \cdot \frac{K_p}{\rho g} \cdot \frac{P_o - P_\infty}{r_o} \qquad (3.14)$$

where P_∞ is the pressure infinitely far away and P_o at the surface of the hemisphere.

It is interesting to note that the above equation says that the entire resistance to flow in the buffer can be imagined to be concentrated in a small tube with buffer. The cross-sectional area of the tube is equal to the area of the hemisphere $\pi \cdot r_s^2 = 2\pi \cdot r_o^2$ and its length is equal to the radius of the hemisphere r_o. This is illustrated in figure 3.5. $r_s = r_o\sqrt{2}$ is obtained from the above.

*This assumption simplifies the mathematical treatment considerably but has little effect on the results otherwise.

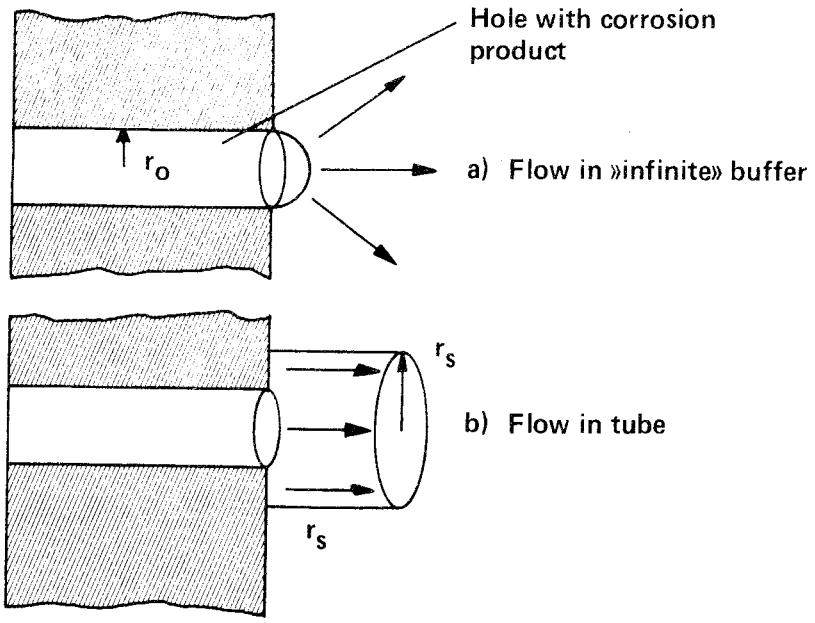

Figure 3.5 Flow from a hole in the canister out into the surrounding buffer. Equivalence between "infinite" buffer a) and a tube with length r_o and cross-section $2\pi r_o^2$ where flow only takes place in the direction of the axis of the tube b).

We now imagine that a fraction x of the area of the hole in the canister consists of pores with an equivalent radius of r_{KAP}. The capillary pressure that drives the water transport is built up in these pores. The outward transport of hydrogen takes place in the large pores, which take up a fraction 1-x of the area. The capillary pressure in the small pores is given by:

$$\Delta P_{KAP} = \frac{2\sigma}{r_{KAP}} \qquad (3.15)$$

The capillary pressure constitutes the driving force for the inward transport of the water. This pressure must be greater than the pressure drop for the flow. Considering the very low hydraulic conductivity of bentonite clay, laminar flow is the only possibility.

According to equation (3.14), the quantity of water that can be transported per unit time is given by:

$$N_{H_2O} = A \cdot x \cdot K_{P_{H_2O}} \cdot \frac{\Delta P_{LAM}}{\rho_{H_2O} \cdot g \cdot r_o} \qquad (3.16)$$

When the water reaches the fuel, hydrogen is formed through radiolysis and the pressure inside the canister increases. The inward transport of water thereby decreases as a result of the rising back-pressure exerted by the hydrogen. The hydrogen is first transported through the corrosion product and then starts to displace the pore water in the buffer material. If this displacement is assumed to take place with a spherical geometry, the hydrogen transport according to equation (3.14) is initially determined by the flow resistance of the water:

$$N_{H_2} = A(1-x) \cdot K_{P_{H_2O}} \cdot \frac{P_2 - P_3}{\rho_{H_2O} \cdot g \cdot r_o} \qquad (3.17)$$

As the water is displaced, the resistance decreases and is finally dominated by the flow resistance of the hydrogen. The relationship (3.17) also applies when the water in the buffer material has been completely displaced and the hydrogen flows freely into the dried-up pores. $K_{P_{H_2O}}$ and P_{H_2O} must, however, be replaced with the values that apply for hydrogen.

A material balance gives the relationship between the volume flow of incoming water and the volume flow of evolved hydrogen:

$$N_{H_2O} = N_{H_2} \cdot \frac{\rho_{H_2}}{\rho_{H_2O}} \cdot \frac{M_{H_2O}}{M_{H_2}} \qquad (3.18)$$

Finally, a pressure balance is required to couple the different transport mechanisms.

$$P_2 - P_3 + \Delta P_{LAM} = \Delta P_{KAP} \qquad (3.19)$$

Table 3.8 shows how the quantity of water transported in is dependent on the area of the hole and the capillary radius for the case where the hydrogen displaces the pore water in the clay. The calculations are carried out for the time at which the water has just begun to be displaced.

The three values that have been assigned to the area of the hole in the canister are 1, 10^2 and 10^4 mm^2 and to the capillary radius 10^1, 10^2 and 10^3 nm.

Table 3.8 Water flow through a hole in the canister wall when the hydrogen pressure inside the canister has been taken into consideration. (The hydrogen displaces the water in the clay.) Unit: moles/year.

	A (mm^2)		
r_{KAP} (nm)	1	10^2	10^4
10^1	$2.5 \cdot 10^{-3}$	$2.5 \cdot 10^{-2}$	$2.5 \cdot 10^{-1}$
10^2	$1 \cdot 10^{-4}$	$1 \cdot 10^{-3}$	$1 \cdot 10^{-2}$
10^3	$8.3 \cdot 10^{-6}$	$8.3 \cdot 10^{-5}$	$8.3 \cdot 10^{-4}$

The same values of the parameters have been used in table 3.9, but the hydrogen does not displace the pore water in the clay, but rather flows freely in the pores.

Table 3.9 Water flow through a hole in the canister wall when the hydrogen pressure inside the canister has been taken into consideration. (The hydrogen flows freely in the clay, the water has already been displaced.) Units: moles/year.

	A (mm^2)		
r_{KAP} (nm)	1	10^2	10^4
10^1	$2 \cdot 10^{-2}$	$2 \cdot 10^{-1}$	2
10^2	$2 \cdot 10^{-3}$	$2 \cdot 10^{-2}$	$2 \cdot 10^{-1}$
10^3	$2 \cdot 10^{-4}$	$2 \cdot 10^{-3}$	$2 \cdot 10^{-2}$

Another interesting quantity in this context is the displacement time. This provides some idea of at what time the hydrogen starts to be transported away by means of flow instead of displacement. The volume of water that is to be displaced is actually infinitely great, which means an infinite displacement time. We have therefore chosen to use the volume generated between two spherical concentric shells with a radius of r_o and $10xr_o$ as an approximation. The pressure drop has then decreased to 90% of the "infinite value". The displacement time has been calculated in this manner for a capillary radius of 10 nm and hole areas of 10^2 and 10^4 mm^2. The results are given in table 3.10.

Table 3.10 Displacement time

r_{KAP} = 10 nm

A_2 (mm^2)	Time (years)
10^2	1
10^4	100

In addition to hydrogen, hydrogen peroxide is formed during radiolysis. Hydrogen peroxide is a strong oxidizing agent that will probably attack the canister material and make additional holes in the canister. This can be envisaged as follows: An initial canister damage has occurred in the form of a 1 mm^2 hole. Water enters via the mechanism described above and is radiolysed. The hydrogen peroxide formed attacks the copper and widens the hole. After 1000 years, the diameter of the hole is 5.5 cm for the case with a capillary radius of 10 mm and a canister thickness of 6 cm, with the hydrogen peroxide production given in table 3.9 of $2 \cdot 10^{-2}$ moles/year. This means that there is a risk that an initial canister damage will be "quickly" aggravated.

4. MIGRATING REDOX FRONT

In addition to hydrogen, hyrogen peroxide is also formed when water is radiolysed. Like the hydrogen, the hydrogen peroxide is transported out from the repository. The chemical environment in the repository is thereby changed from a reducing to an oxidizing one owing to the oxidizing capacity of hydrogen peroxide. It is then primarily the iron present in the buffer material and in the surrounding rock that determines the redox potential. As long as bivalent iron is present, the environment is considered to be reducing. The environment is considered to be oxidizing when iron is in the trivalent state. The scenario we postulate is the following: A hole has been created in the canister wall through which water enters and is distributed in the canister. When it comes into contact with the spent fuel, radiolysis occurs. The hydrogen peroxide formed in this manner diffuses out into the buffer material. Where it comes into contact with bivalent iron, the latter is oxidized to trivalent iron. Since the reaction is instantaneous, a sharp boundary is created between regions with an oxidizing and a reducing environment. As the radiolysis progresses and produces more hydrogen peroxide, this front moves farther away from the cansiter.

4.1 Front propagation without diffusional resistances

If the diffusional resistances are neglected, the location of the front at different points in time can be calculated by means of a material balance. In this material balance, the quantity of hydrogen peroxide formed is set equal to twice the quantity of bivalent iron according to the reaction $H_2O_2 + 2Fe^{2+} + 2H^+ = 2Fe^{3+} + 2H_2O$. The underlying assumptions are summarized below.

* The surface of all fuel pellets in 499 rods is in direct contact with water.

* The inward transport of water does not constitute a limiting factor.

* The reaction between bivalent iron and hydrogen peroxide is instantaneous.

* All diffusional resistances are neglected.

* The entire measured quantity of iron in the bentonite and granite is accessible to the hydrogen peroxide.

* The hydrogen peroxide diffuses only in the radial direction.

With radial propagation, the location of the front is obtained from:

$$r_m = \sqrt{\frac{m_{ox}}{\pi \cdot L \cdot C_L} + r_1^2} \qquad (4.1)$$

for $r_m < r_2$

and for $r_m > r_2$, the following is obtained:

$$r_m = \sqrt{\frac{1}{C_G}\left\{\frac{m_{ox}}{\pi \cdot L} - r_2^2\,(C_L - C_G) + r_1^2 \cdot C_L\right\}} \qquad (4.2)$$

The location of the front is given in the tables below at different points in time. Canister breakthrough is assumed to take place after 40 and 10^5 years, respectively.

Table 4.1 Migration distance of redox front due to hydrogen peroxide formed by α-radiolysis. (Canister breakthrough after 40 years.)

Time (years)	Location of front (from centre of canister) (m)
10^2	0.8
10^3	1.3
10^4	2.3
10^5	3.6
10^6	4.6

Table 4.2 Migration distance of redox front due to hydrogen peroxide formed by α-radiolysis. (Canister breakthrough after 10^5 years.)

Time (years)	Location of front (from centre of canister) (m)
10^6	3.0

The results in tables 4.1 and 4.2 are based on the following data:

C_L = 19.2 moles/m^3 (see reference (14)) (density of bentonite: 1800 kg/m^3)
C_G = 136 moles/m^3 (see reference (14)) (density of granite: 2700 kg/m^3)
r_1 = 0.375 m r_2 = 0.75 m
L = 5 m

As is evident from the table, the redox front reaches beyond the clay barrier relatively quickly. Another transport mechanism whereby the hydrogen peroxide can be dispersed is thereby added, namely convection in the water-bearing fractures. This has been dealt with in detail by Neretnieks (15).

4.2 Front propagation with diffusional resistances in clay and rock

The preceding section dealt with the propagation of the front when the diffusional resistances are neglected. In the following calculations, the diffusional resistances are included, but the water flow in the fractures is still neglected. The hydrogen peroxide is still assumed to be emitted by the entire canister surface and it diffuses only in the radial direction. The movement of the front is described by the following equations. The concentration profile between the canister ($r = r_1$) and the redox front ($r = r_m$) is obtained from the diffusion equation:

$$D_p \cdot \frac{1}{r} \frac{\partial}{\partial r} \left(r \frac{\partial c}{\partial r}\right) = \frac{\partial c}{\partial t} \qquad (4.3)$$

The migration velocity of the front is obtained by setting the flow of hydrogen peroxide at the front face equal to the amount of iron consumed per unit time, i.e.

$$-D_p \cdot \varepsilon_p \cdot \frac{\partial c}{\partial r}/_{r=r_m} = (1 - \varepsilon_p) \cdot q_o \cdot \frac{dr_m}{dt} \qquad (4.4)$$

The equations (4.3) and (4.4) have the same fundamental appearance for both the clay and the rock, but the constants D_p, ε_p and q_o have different values depending on different material properties.

Boundary and initial conditions

$$c = 0 \qquad r = r_m \qquad \text{alla } t \qquad (4.5)$$

$$c = 0 \qquad \text{alla } r \qquad t = 0 \qquad (4.6)$$

Since hydrogen peroxide production in the canister is dependent on time (11) the boundary condition at the canister surface ($r = r_1$) is time-dependent. It is written as:

$$-D_p \cdot \varepsilon_p \cdot 2\pi \cdot r_1 \cdot L \cdot \frac{\partial c}{\partial r}/_{r=r_1} = P(t) \qquad (4.7)$$

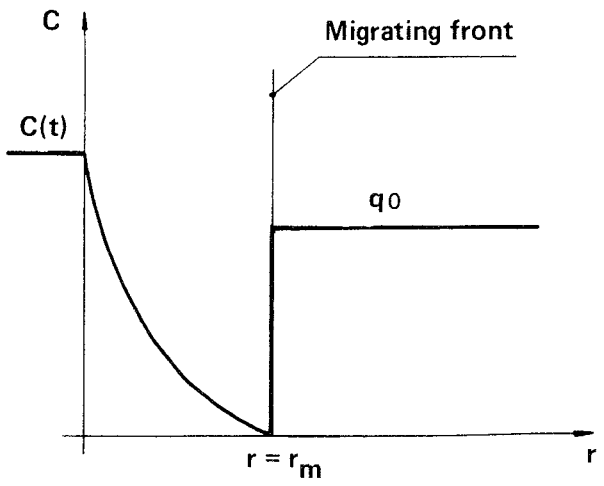

Figure 4.1 Migrating redox front

Where P(t) is the production rate, which varies according to the table below:

Table 4.3 Hydrogen peroxide production due to α-radiolysis as a function of time. (Canister breakthrough after 40 years.)

Time (years)	Production rate (moles/year)
40	2.6
100	2.4
300	1.6
600	0.9
10^3	0.66
10^4	0.17
10^5	0.013
10^6	0.005

The production rates for intervening times in table 4.3 were obtained by means of linear interpolation.

Equations (4.3) - (4.7) were solved numerically with the computer program TRUMP (7). The results are given in table 4.4. A comparison between analytical solution and TRUMP solution is presented in appendix 1.

Table 4.4. Propagation of the redox front with diffusional resistances in clay and rock.

Time (years)	Distance of front from centre of canister (m)	Highest concentration of H_2O_2 in pore water in clay (moles/l)
10^3	1.1	1.3
10^4	1.9	2.3
10^5	3.6	0.71

Data used:

Rock

$D_p \cdot p = 10^{-13}$ m^2/s

$p = 10^{-3}$

$C_G = 136$ moles/m^3

Clay

$D_p \cdot p = 10^{-10}$ m^2/s

$p = 10^{-1}$

$C_L = 19.2$ moles/m^3

4.3 Comparison between transport into the rock matrix and to a fracture with flowing water

When the redox front has penetrated the clay barrier, the hydrogen peroxide can be transported further in the rock either by diffusion in the rock matrix or by convection in the water-bearing fractures. Which of these mechanisms is the dominant one can be estimated in the following manner: For a given driving force (concentration difference), the transport rate can be approximated by

$$N = - D_e \cdot A \cdot \frac{\Delta c}{\Delta x} \qquad (4.8)$$

where Δx is the migration distance of the front in the rock.

Transport to the flowing water in the fractures can be expressed in the form of an equivalent water flow (U_{eq}) and a concentration difference.

$$N = U_{eq} \cdot \Delta c \qquad (4.9)$$

Now the thickness Δx can be calculated when the transport rates are equal with the two mechanisms.

$x = 0.19$ m is obtained with the following data.

$D_e = 10^{-13}$ m^2/s (see reference (17, 18))
$U_{eq} = 0.45$ l/year (see reference (19))
$A = 28$ m^2

This means that when the redox front has migrated further than 0.19 m in the rock matrix, the flow in the fractures will dominate. In order to oxidize this distance in the rock, 266 moles of hydrogen peroxide are required. The propagation of the redox front taking water flow into consideration is dealt with in greater detail by Neretnieks (15).

4.4 Discussion and conclusions

The altered redox conditions that can arise in the near field in connection with a canister breakthrough depend solely on α-radiolysis. The good shielding offered by the proposed canister thicknesses enables the γ-radiolysis to be completely neglected in this case. In the calculations reported here, a rather conservative value of the exposed fuel area has been used. The surface area of all fuel pellets in 499 rods has been used here. In the extreme case, a larger exposed area can be imagined if the pellets are completely or partially dissolved into smaller particles. Together with the dose rate, the fuel area that is in contact with the water determines the rate of radiolysis. Radiolysis then increases considerably.

It has also been assumed that hydrogen peroxide is emitted from the entire surface of the canister, as a consequence of which the front propagates symmetrically in the radial direction. This must be considered highly unlikely. It is more probable that the canister damage take the form of one or more holes in the copper wall. This case cannot be simulated, unfortunately, owing to the large number of nodes required to represent the three-dimensional geometry with

sufficient accuracy. The number is so great that the computer currently being used does not have a sufficient memory capacity. In order for it to be possible to carry out such calculations, the TRUMP program (15) must be transferred to a larger computer. In view of the uncertainties in input data that currently exist, it is doubtful whether the improvement of the calculation method would be significant. Until the uncertainties have been eliminated, the methods used provide a sufficiently good estimate.

The simple approximate calculations, in which the diffusional resistances have been neglected, show that the bivalent iron in the clay is consumed relatively quickly. The flow of water in the rock fractures will thereby contribute to the dispersion of hydrogen peroxide. Simultaneously with this convective transport, diffusion takes place in the micropores in the rock matrix. The result is that the fracture faces are oxidized first, after which the oxidation front moves further into the rock. This transport pathway, from the canister via the buffer and rock fractures into the rock matrix, is the same as that taken by radionuclides from a leaking canister. This eliminates the previously good retardation conditions in a reducing environment.

5. NOTATIONS

A	area	(m^2)
b	half the fracture width	(m)
c	concentration	$(kmol/m^3)$
C_L	iron content of clay	$(kmol/m^3)$
C_G	iron content of rock	$(kmol/m^3)$
C_{TOT}	total concentration	$(kmol/m^3)$
D_p	diffusivity in pores	(m^2/s)
D_v	diffusivity in water	(m^2/s)
D_L	longitudinal dispersion coefficient	(m^2/s)
g	gravitational constant	(m/s^2)
h	height	(m)
i	hydraulic gradient	(m/m)
k	mass transfer coefficient	(m/s)
K	total mass transfer coefficient	(m/s)
K_p	hydraulic conducitvity	(m/s)
L	length of canister	(m)
M	molar weight	(kg/kmol)
N	rate of mass flow	(kmol/s)
P	pressure	(Pa)
P_2	hydrogen pressure inside canister	(Pa)
P_o, P_3	static pressure	(Pa)
Q	flow	(m^3/s)
r	radial coordinate	(m)
r_1	outer radius of canister	(m)
r_m	location of front	(m)
r_2	outer radius of clay barrier	(m)
R_{TOT}	total resistance (= 1/KA)	(s/m^3)
R_L	resistance in clay	(s/m^3)

R_V	resistance between clay and groundwater	(s/m^3)
r_s	equivalent radius	(m)
r_{KAP}	capillary radius	(m)
R	universal gas constant	(J/mol,K)
S	fracture spacing	(m)
T	temperature	(K)
t	time	(s)
t_k	contact time	(s)
u_o	bulk velocity of groundwater	(m/s)
U_{eq}	equivalent water flow	(m^3/s)
V_r	component of velocity field in r direction	(m/s)
V	component of velocity field in direction	(m/s)
x	mole fraction	(kmol/kmol)
z	coordinate in longitudinal direction of canister	(m)
ρ	density	(kg/m^3)
σ	surface tension	(N/m)
θ	angular coordinate	(radians)

6. REFERENCES

(1) Neretnieks I., "Transport of oxidants and radionuclides through a clay barrier", KBS Teknisk Rapport Nr 79, (1978).

(2) "Handling and Final Storage of Unreprocessed Spent Nuclear Fuel", Vol. II, KBS Teknisk Rapport (1978).

(3) Neretnieks I., "Retardation of escaping nuclides from a final depository", KBS Teknisk Rapport nr 30, (1977).

(4) Bird, et.al., "Transport Phenomena", Wiley & Sons, Inc, (1960).

(5) Crank J., "The Mathematics of Diffusion", 2nd ed., Clarendon Press, (1975).

(6) "Handbook of Chemistry and Physics", 60th ed., CRC Press, (1980).

(7) Edwards A.L., "TRUMP: A Computer Program for Transient and Steady State Temperature Distribution in Multi-dimensional Systems", National Technical Information Service, National Bureau of Standards, Springfield, Va., USA. (1972).

(8) Rasmuson A., Narasimhan T.N. and Neretnieks I., "Chemical transport in a fissured rock: Verification of a numerical model", Water Resources Research in press (1982).

(9) Perry R.H., Chilton C.J., "Chemical Engineers' Handbook" 5th edition Mc Graw-Hill.

(10) Christensen H., Bjergbakke E., "Radiolysis of Ground Water from HLW Stored in Intact Copper Canisters", Technical Report, Studsvik (1982).

(11) Christensen H., Bjergbakke E., "Radiolysis of Ground Water from HLW Stored in Copper Canisters", Technical Report, Studsvik (1982).

(12) Neretnieks I., Skagius C., "Diffusivitetsmätningar av metan och väte i våt lera", KBS Teknisk Rapport nr 86, (1978).

(13) Pusch R., "Highly compacted Na bentonite as buffer substance", KBS Teknisk Rapport nr 74, (1978).

(14) Torstenfeldt B., Personal Communication, 1982

(15) Neretnieks I., "A Note on the Movement of a Redox Front Downstream from a Repository for Nuclear Waste" (1982).

(16) Carslaw H.S. and Jaeger J.C., "Conduction of Heat in Solids", 2nd ed., Oxford University Press, 1959.

(17) Skagius K., Neretnieks I., "Diffusion in Crystalline Rocks", Department of Chem. Eng., Paper presented at the "Fifth International Symposium on The Scientific Basis for Radioactive Waste Management", Berlin June 1982, Proceedings.

(18) Skagius C., Svedberg G., Neretnieks I., "A Study of Strontium and Cesium Sorption on Granite". Report No. 4.26 National Council for Radioactive Waste, PRAV, Stockholm, Sweden 1981.

(19) Neretnieks I., "Leach Rates of High Level Waste and Spent Fuel - Limiting Rates as determined by Backfill and Bedrock Conditions", Paper presented at the "Fifth International Symposium on the Scientific Basis for Nuclear Waste Management", Berlin June 1982, Proceedings.

(20) Allard B., "Solubilities of Actinides in Neutral or Basic Solutions", Proc. Actinides 81, Asilomar Sept 1981 in press.

Appendix
1(3)

Comparison between analytical and TRUMP solution of a migrating front problem

A substance A diffuses in a medium that only contains substance B at the start. A and B react instantaneously and irreversibly with each other according to the formula A + B -> products. Owing to the reaction, the two substances cannot be present simultaneously at a single point. A sharp front will therefore be formed between a region with only A and another with only B. See fig. 1. As B is consumed, the location of the front will change.

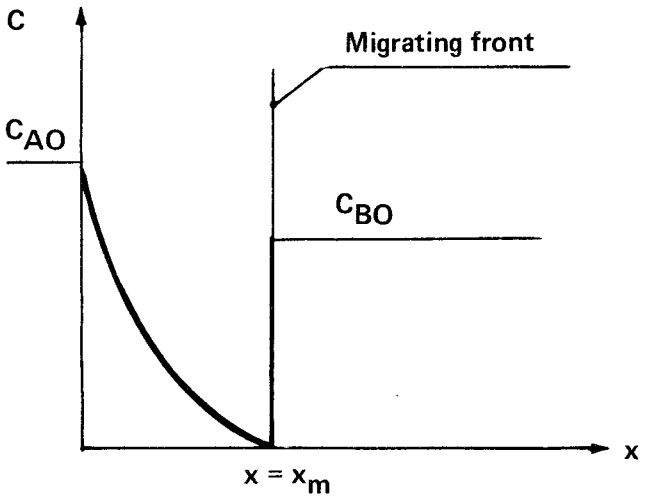

Figure 1.

The concentrations at the front face of A are equal to zero. In our case, where we assume that the reducing agent Fe(II) is bound in the rock and the clay, the diffusivity of B is also equal to zero. This means that the concentration in the region with B only is constant ($=C_{BO}$).

The concentration profile for component A between the boundary ($x = 0$) and the front ($x = x_m$) is obtained from:

$$D_A \frac{\partial^2 c_A}{\partial x^2} = \frac{\partial c_A}{\partial t} \qquad (1)$$

for diffusion in one direction with the following boundary and initial conditions

$c_A = c_{AO}$ $\quad x = 0$ $\quad$ alla t

$c_A = 0$ $\quad x = x_m$ $\quad$ alla t

$c_A = 0$ $\quad$ alla x $\quad t = 0$

The migration rate of the front is obtained by setting the flow of A at the front face equal to the quantity B consumed per unit time, i.e.

$$-D_A \cdot \frac{\partial c_A}{\partial x}\Big|_{x=x_m} = c_{BO} \cdot \frac{dx_m}{dt} \qquad (2)$$

with the initial condition

$$x_m = 0 \qquad t = 0$$

An analytical solution to this "moving boundary" problem is reported in the literature ((5) p. 298).

The location x_m of the front as a function of time is obtained from:

$$x_m = \alpha \cdot \sqrt{4D_A \cdot t} \qquad (3)$$

where α is the root of the equation:

$$\frac{c_{BO}}{c_{AO}} \cdot \sqrt{\pi} \cdot \alpha \cdot e^{\alpha^2} \cdot \mathrm{erf}\,(\alpha) = 1 \qquad (4)$$

The concentration profile for component A for $0 < x < x_m$ is obtained by:

$$c_A = c_{AO} \cdot \left(1 - \frac{\mathrm{erf}\,(x/\sqrt{4D_A t})}{\mathrm{erf}\,(\alpha)}\right) \qquad (5)$$

Table 1 presents values of the concentration profile between $x = 0$ and $x = x_m$ at the time 59.2 years with the following values of the parameters:

$$D_A = 3 \cdot 10^{-3} \text{ m}^2/\text{year}; \; c_{AO} = 10 \text{ g/m}^3; \; c_{BO} = 10 \text{ g/m}^3.$$

Table 1. Comparison between analytical and TRUMP solution at t = 59.2 years

x (m)	C_A	
	Analytical solution	TRUMP solution
0.0	10.0	10.0
0.05	8.92	8.90
0.15	6.79	6.73
0.25	4.75	4.70
0.35	2.85	2.89
0.45	1.12	1.35

FÖRTECKNING ÖVER KBS TEKNISKA RAPPORTER

1977-78

TR 121 KBS Technical Reports 1 - 120.
Summaries. Stockholm, May 1979.

1979

TR 79-28 The KBS Annual Report 1979.
KBS Technical Reports 79-01--79-27.
Summaries. Stockholm, March 1980.

1980

TR 80-26 The KBS Annual Report 1980.
KBS Technical Reports 80-01--80-25.
Summaries. Stockholm, March 1981.

1981

TR 81-17 The KBS Annual Report 1981.
KBS Technical Reports 81-01--81-16
Summaries. Stockholm, April 1982.

1982

TR 82-01 Hydrothermal conditions around a radioactive waste repository
Part 3 - Numerical solutions for anisotropy
Roger Thunvik
Royal Institute of Technology, Stockholm, Sweden
Carol Braester
Institute of Technology, Haifa, Israel
December 1981

TR 82-02 Radiolysis of groundwater from HLW stored in copper canisters
Hilbert Christensen
Erling Bjergbakke
Studsvik Energiteknik AB, 1982-06-29

TR 82-03 Migration of radionuclides in fissured rock:
Some calculated results obtained from a model based on the concept of stratified flow and matrix diffusion
Ivars Neretnieks
Royal Institute of Technology
Department of Chemical Engineering
Stockholm, Sweden, October 1981

TR 82-04 Radionuclide chain migration in fissured rock -
The influence of matrix diffusion
Anders Rasmuson *
Akke Bengtsson **
Bertil Grundfelt **
Ivars Neretnieks *
April, 1982

* Royal Institute of Technology
Department of Chemical Engineering
Stockholm, Sweden

** KEMAKTA Consultant Company
Stockholm, Sweden

TR 82-05 Migration of radionuclides in fissured rock -
Results obtained from a model based on the concepts of hydrodynamic dispersion and matrix diffusion
Anders Rasmuson
Ivars Neretnieks
Royal Institute of Technology
Department of Chemical Engineering
Stockholm, Sweden, May 1982

TR 82-06 Numerical simulation of double packer tests
Calculation of rock permeability
Carol Braester
Israel Institute of Technology, Haifa, Israel
Roger Thunvik
Royal Institute of Technology
Stockholm, Sweden, June 1982

TR 82-07 Copper/bentonite interaction
Roland Pusch
Division Soil Mechanics, University of Luleå
Luleå, Sweden, 1982-06-30

TR 82-08 Diffusion in the matrix of granitic rock
Field test in the Stripa mine
Part 1
Lars Birgersson
Ivars Neretnieks
Royal Institute of Technology
Department of Chemical Engineering
Stockholm, Sweden, July 1982

TR 82-09:1 Radioactive waste management plan
PLAN 82
Part 1 General
Stockholm, June 1982

TR 82-09:2 Radioactive waste management plan
PLAN 82
Part 2 Facilities and costs
Stockholm, June 1982

TR 82-10 The hydraulic properties of fracture zones and tracer tests with non-reactive elements in Studsvik
Carl-Erik Klockars
Ove Persson
Geological Survey of Sweden, Uppsala
Ove Landström
Studsvik Energiteknik, Nyköping
Sweden, April 1982

TR 82-11 Radiation levels and absorbed doses around copper canisters containing spent LWR fuel
Klas Lundgren
ASEA-ATOM, Västerås, Sweden 1982-08-11

TR 82-12 Diffusion in crystalline rocks of some sorbing and nonsorbing species
Kristina Skagius
Ivars Neretnieks
Royal Institute of Technology
Department of Chemical Engineering
Stockholm, Sweden, 1982-03-01

TR 82-13 Variation in radioactivity, uranium and radium-226 contents in three radioactive springs and along their out-flows, northern Sweden
John Ek
Sverker Evans
Lennart Ljungqvist
Studsvik Energiteknik AB
Nyköping, Sweden, 1982-06-03

TR 82-14 Oral intake of radionuclides in the population
A review of biological factors of relevance for assessment of absorbed dose at long term waste storage
Lennart Johansson
National Defense Research Institute, Dept 4
Umeå, Sweden, October 1982

TR 82-15 Radioactive disequilibria in mineralised drill core samples from the Björklund uranium occurrence, northern Sweden
J A T Smellie
Geological Survey of Sweden
Luleå, December 1982

TR 82-16 The movement of a redox front downstream from a repository for nuclear waste
Ivars Neretnieks
Royal Institute of Technology
Stockholm, Sweden, 1982-04-19

TR 82-17 Diffusion of hydrogen, hydrogen sulfide and large molecular weight anions in bentonite
Trygve E Eriksen
Department of Nuclear Chemistry
Royal Institute of Technology, Stockholm
Arvid Jacobsson
Division of Soil Mechanics
University of Luleå
Sweden, 1982-07-02

TR 82-18 Radiolysis of ground water from spent fuel
Hilbert Christensen
Erling Bjergbakke
Studsvik Energiteknik AB
Nyköping, Sweden, 1982-11-27

TR 82-19 Corrosion of steel in concrete
Carolyn M Preece
Korrosionscentralen
Glostrup, Denmark, 1982-10-14

TR 82-20 Fissure fillings from Finnsjön and Studsvik, Sweden
Identification, chemistry and dating
Eva-Lena Tullborg
Sven Åke Larson
Swedish Geological, Gothenburg
December 1982

TR 82-21 Sorption of actinides in granitic rock
B Allard
Department of Nuclear Chemistry
Chalmers University of Technology
Göteborg, Sweden 1982-11-20

TR 82-22 Natural levels of uranium and radium in four potential areas for the final storage of spent nuclear fuel
Sverker Evans
Svante Lampe
Björn Sundblad
Studsvik Energiteknik AB
Nyköping, Sweden, 1982-12-21

TR 82-23 Analysis of groundwater from deep boreholes in Kråkemåla, Sternö and Finnsjön
Sif Laurent
IVL
Stockholm, Sweden 1982-12-22

TR 82-24 Migration model for the near field
Final report
Göran Andersson
Anders Rasmuson
Ivars Neretnieks
Royal Institute of Technology
Department of Chemical Engineering
Stockholm, Sweden 1982-11-01